Energy Sources, Part A, 29:1–19, 2007

ISSN: 1556-7036 print/1556-7230 online
DOI: 10.1080/15567030600968648

Taylor & Francis
Taylor & Francis Group

Evolution of the Earth's Global Climate

O. G. SOROKHTIN

Laboratory at the Institute of Oceanology of Russian Academy of Sciences
Moscow, Russia

G. V. CHILINGAR

Rudolf W. Gunnerman Energy and Environment Laboratory
University of Southern California
Los Angeles, California, USA

L. KHILYUK

Russian Academy of Natural Sciences, USA Branch
Los Angeles, California, USA

M. V. GORFUNKEL

Russian Academy of Natural Sciences, USA Branch
Dallas, Texas, USA

Abstract *The model of the Earth's climate change described here is based on the Earth's global evolution theory and adiabatic theory of the greenhouse effect. The main factor determining climate's temperature parameters is the atmospheric pressure. Glaciations at the end of Paleozoic–Phanerozoic time occurred due to a gradual atmospheric pressure decline as a result of nitrogen consumption by the nitrogen-consuming bacteria that removed nitrogen from the atmosphere and concentrated it in sediments. A warm period in the second half of Mesozoic was associated with the formation of the Pangaea supercontinent and intensified oxygen generation, which compensated for the lowered nitrogen partial pressure.*

Keywords adiabatic theory, climate evolution, global warming, greenhouse gases

Introduction

Earth is the only planet in the solar system with a unique atmosphere providing a climate favorable for the development of highly organized life forms. That occurred due to numerous circumstances: (1) Sun is a "quiescent" star; (2) Earth is located at the optimum distance from the Sun; (3) Earth has a massive satellite, the Moon; and (4) chemical composition of the primordial Earth. Climatic conditions favorable for life were in particular

Address correspondence to George Chilingar, 101 Windsor Blvd., Los Angeles, CA, USA 90004. E-mail: gchiling@usc.edu

due to strong feedback between the evolution of the Earth's biota and the development of the atmosphere.

A very important factor defining the climatic conditions on Earth is its surface temperature. Temperatures of the past geologic epochs may be deduced from oxygen isotope ratios; for example, in the marine silica that usually formed in equilibrium with the surrounding water. The $\delta^{18}O$ values in marine silica substantially depend on the water temperature of their depositional environment. Based on laboratory determinations, it is usually believed that the temperature in the atmosphere increased at least 3.4 BY ago (Perry and Tan, 1972). By mid-Archaean time, the $\delta^{18}O$ values in the Onverwacht chert of Greenstone Formation (South Africa) declined to +18–+21‰ (current values are +32‰). This suggests a rise in the oceanic water temperature during Middle Archaean time to +70°C (Knauth and Lowe, 1978). Some other studies indicate that in mid-Archaean time, 3.2 BY ago, the oceanic water temperature may have reached +90°C (Perry, 1967). The isotope composition of siliceous schist from the same Barberton Belt may have reached +70 to +100°C (Perry, 1967). Indeed, as temperature increases, the $\delta^{18}O$ value in SiO_2 must decline. For instance, for $\delta^{18}O$ value in $SiO_2 \approx 15‰$, at the zero value of $\delta^{18}O$ in the marine water, the SiO_2 formation temperatures must be substantially above +100°C, whereas the water temperature corresponding to $\delta^{18}O \approx 32‰$ is about +20°C.

It is not totally clear, however, as to what extent the $\delta^{18}O$ value in the ancient silica deposits is related to their origin, and especially the temperature of the water in which they were formed (Holland, 1984; Schopf, 1980). It is quite possible that a decline in $\delta^{18}O$ value with time observed in SiO_2 was associated not only with changes in the ocean water temperature but also is due to other causes. Among these may have been the degassing of water from mantle previously not accounted for (this water contains iron and its oxides). It may have been the reactions between the water and its dissolved bivalent iron compounds and carbon dioxide, which also resulted in regularity in the decline of $\delta^{18}O$ values in Archaean ocean waters (Sorokhtin and Ushakov, 2002):

$$H_2^{18}O + Fe(HC^{16}O_3) \rightarrow H_2^{16}O + Fe(HC^{18}O^{16}O_2)_2 + 2.34 \text{ kcal/g } (H_2O), \quad (1)$$

$$H_2^{18}O + C^{16}O_2 \rightarrow H_2^{16}O + C^{18}O^{16}O + 0.9 \text{ kcal/g } (H_2O) \quad (2)$$

A similar exchange reaction occurred during hydration of oceanic crust rocks and during formation of silica:

$$H_2^{18}O + Si^{16}O_2 \rightarrow H_2^{16}O + Si^{18}O^{16}O + 1.59 \text{ kcal/g } (H_2O) \quad (3)$$

In the process, the SiO_2 became isotopically heavier. However, as the isotopic composition of ocean water became significantly lower during the Early Pre-Cambrian time, the ancient isotopic composition of SiO_2 also became lighter compared with the modern ones.

The writers estimate that due to the effect of reactions similar to (1) through (3), the $\delta^{18}O$ value of marine water during the Early Archaean time decreased to $\approx -10‰$, whereas the current $\delta^{18}O = 0$. In this case, the Early Archaean sea water temperature would have been much more moderate—no higher than +60°C. Figure 1 shows not only the $\delta^{18}O$ distribution in marine silica of different age, but also the respective seawater temperature. The Earth's surface temperature at the sea level was continuously declining beginning in the Archaean time despite the fact that luminosity of Sun at that time

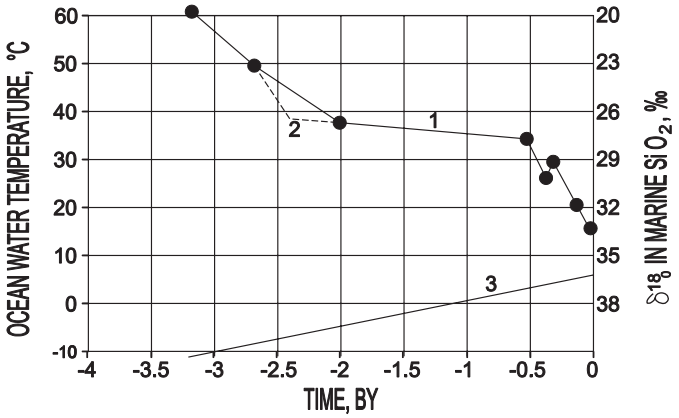

Figure 1. Curve 1—Isotope temperature of the marine SiO_2 of different geologic ages (left Y-axis) and corresponding δ^{18}O oxygen values versus the SMOW standard (right Y-axis). It is assumed that the δ^{18}O value of the Archaean marine water was $\approx -10‰$, whereas for the Phanerozoic and present-day marine water $\delta^{18}\mathrm{O} = 0$. The solid dots are by T. Schopf (1980) with corrections. Curve 2—Likely temperature and δ^{18}O distribution over the interval where data are missing in Schopf's publication. Curve 3—Temperature of the absolute black body characterizing the increase in Sun's luminosity with time.

was approximately 20 to 30% lower that the present-day one and was only gradually increasing to the present-day level (Bachall, 1982). This is an important paradox that needs to be explained.

According to the adiabatic theory of greenhouse effect (see below), besides the Sun's radiation, the main determining factors of the Earth's climate are the Earth's atmosphere pressure and its composition. The denser the atmosphere (i.e., the higher the atmospheric pressure), the warmer the climate. Thus, the high surface temperature at the ocean level during the Archaean time, at a low Sun's luminosity, may only be a result of higher atmospheric pressure. The gradual decrease in the oceanic water temperature with a smooth increase of Sun's luminosity may only be a result of a gradual decrease in the atmospheric pressure. As shown later, the temperature will continue to drop in the future.

Recently, it became popular to profess a substantial warming of global climate caused by human economic activity (through venting into the atmosphere of the so-called greenhouse gases, mostly carbon dioxide and methane). The concept of an atmospheric heating due to greenhouse gases had been first presented by Svante Arrhenius (1896). Since then, it was accepted as self-evident, practically with no verification (Budyko, 1997; Global Warming, 1990; Greenhouse Effect, 1989). This approach totally dominates the conclusions by the Intergovernmental Panel on Climate Change (IPCC); Greenpeace; UN Environmental Program; and World Meteorological Organization.

The same approach had been totally supported by International Environmental Congresses in Rio de Janeiro, Brazil (1992) and in Kyoto, Japan (1997). Forecasts of the proponents predict a temperature increase by 2.5°C to 5°C by the year 2100 and the resulting ocean level rise of 0.6 to 1 m. Some recent studies of the Greenland ice cover came to even more alarming conclusions. That would cause substantial problems for densely populated continental coastal areas all over the low-land areas. Other fatal consequences include desert expansion, permafrost melting and disappearance, and erosion of soil.

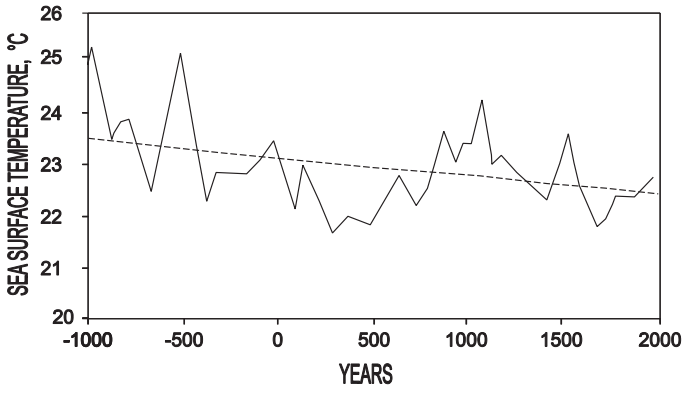

Figure 2. Surface temperature in the Sargasso Sea (averaged over 50-year periods) as determined from oxygen isotope ratios in the marine plankton remains of the seafloor deposits (Kegwin, 1996). 23°C is the average over a 3,000-year period.

How Justified Is that Finding? Aren't We Fighting the Windmills?

The currently observed global warming began early in XVIIth century when there were no significant technogenic carbon dioxide gas releases to the atmosphere. A more global outlook is provided in: "Northern Hemisphere Summer Temperatures of the Last Six Centuries" by K. R. Briffa, P. D. Jones, F. H. Schweingruber, and T. J. Osborn (1998). They suggest that the latest warming trend began around 1850, at the end of the so-called "Little Ice Age" and about the time when technological development greatly accelerated. This acceleration, however, could not have caused any climatic changes as it had been too slight compared to what is going on now.

The current warming appears to be occurring against the backdrop of a general long-term cooling (Figure 2). As for the warming during the recent decades (if it is real), it may turn out to be a temporary phenomenon against the background of the general long-term climate change.

A general temperature decline is also observed in the near-seafloor (bottom) water (Figure 3).

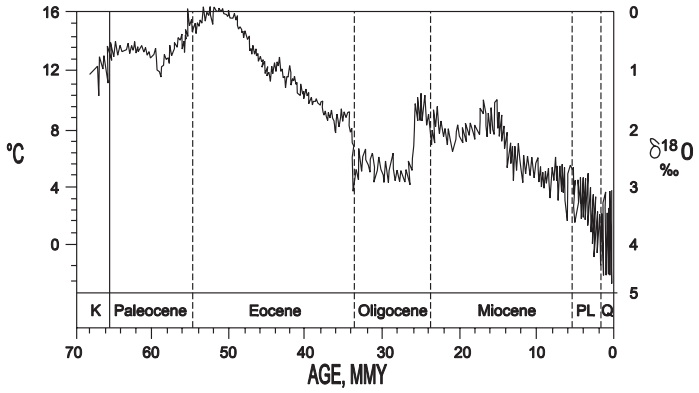

Figure 3. Deep oceanic water temperature based on oxygen ^{18}O isotope ratios in benthos fauna of carbonates (after Zachos et al., 2001; the temperature scale presented by the writers).

The World Ocean near-bottom water temperature decline is associated with the Cenozoic Earth's climate cooling and emergence (38 to 40 MMY ago) in the Antarctic of first glaciers and their broad expansion during the Oligocene time and later. During the Pliocene and Quaternary time, the glaciation of Arctic regions began, which resulted in the temperature decline to almost 0°C in the near-bottom water.

In order to make a qualitative estimate of possible climatic fluctuations, it is necessary to examine the adiabatic theory of greenhouse effect as well as to identify all possible natural causes affecting changes in the temperature of Earth's surface and of troposphere.

The Adiabatic Theory of Greenhouse Effect

Up to the 1990s, there was no theory on the greenhouse effect. All calculations of the effect of CO_2 and other greenhouse gases on Earth's climate were conducted using various intuitive, often prejudicial models.

Inasmuch as the Earth's atmosphere is clearly a dissipative system that is described by nonlinear equations of mathematical physics, the writers used a synergistic approach in analyzing the problem of the self-organizing physical fields and the formation of stable thermodynamic structures (on the time and space scale), determined by the process parameters.

Using this approach, one can use only the most significant and reliably established medium parameters and definable characteristics of the controlling process. For example, one can use only such parameters as the atmospheric mass and its heat capacity, and the average value of incident solar radiation energy. Also, a strong negative relationship between the planet's spherical albedo and its averaged near-surface temperature must be taken into account. As a result, the local details of greenhouse effect are lost because the first approximation model is one-dimensional and averaged over the entire Earth.

Earth is the only solar system's planet with a unique atmosphere and hydrosphere favorable for the development on Earth' surface of highly organized life forms. According to our theory of the greenhouse effect, the main factors determining the comfortable climatic conditions on Earth were the amount of the solar radiation and pressure and the heat capacity of atmosphere (Sorokhtin, 2001). According to our theory, the near-surface temperature T_s and the temperature T at any level in the troposphere is proportional to the temperature of a revolving absolute black body (T_{bb}) at a distance equal to the distance between the Sun and Earth. The latter temperature depends on the Sun's radiation intensity (constant) $S = 1.3672 * 10^6$ erg/cm^2 $*$ s, atmospheric pressure p to the power of adiabatic coefficient α, which depends on the composition of atmosphere and its heat capacity:

$$T = b^{\alpha} * T_{bb} * p^{\alpha} = b^{\alpha} * \left(\frac{S}{4\sigma}\right)^{1/4} * p^{\alpha}, \tag{4}$$

where σ is the Boltzmann's constant ($5.67 * 10^{-5}$ erg/cm^2 $*$ s $*$ deg^{-4}); $\alpha = (\gamma - 1)/\gamma$ and $\gamma = c_p/c_v$ (c_p and c_v are, respectively, specific heats of air at a constant pressure and a constant volume; and b is the scale proportionality coefficient (1.186 atm^{-1}), which varies inversely with pressure (it is constant when the precession angle of the revolving planet is constant). The Sun's constant in the above equation is divided by 4 because the Earth's disk illuminated by the Sun is $\frac{1}{4}$ of the total surface of the Earth.

Equation (4) represents the classic version of temperature dependence on the Sun's constant and atmospheric pressure for the case when the precession angle $\psi = 0$.

The precession angle is the angle between the planet's revolution axis and a perpendicular to the ecliptic plane. If the precession angle is not equal to zero, Eq. (4) becomes more complex (Sorokhtin, 2005a):

$$T = \left[\frac{S}{\sigma \left(\frac{\pi/2 - \psi}{\pi/2} * 4 + \frac{\psi}{\pi/2} * 2 * 2 * \frac{1 - \cos\psi}{(\sin\psi)^2} \right)} \right]^{1/4} \left(\frac{p}{p_0} \right)^{\alpha}, \qquad (5)$$

where p_0 is the pressure at sea level ($p_0 = 1$ atm). On inserting the precession angle $\psi = 23.44°$, the average temperature of Earth's surface is the temperature of an "absolute gray" body at a distance of the Earth from Sun: $T_{gb} = 288.2$ K = 15°C.

Our adiabatic theory can be verified by comparing the theoretical and the actual temperature distributions in the tropospheres of Earth and Venus. Thus, it is necessary to determine the values of adiabatic exponent in the atmospheres of Earth and Venus using Earth's atmosphere parameters: $(T_s)_0 = 288.2$ K and $p_0 = 1$ atm. For example, using Eq. (5) the adiabatic exponent α at an elevation of 5 km ($T_{5\,\mathrm{km}} = 255.5$ K and $p_{5\,\mathrm{km}} = 0.5333$ atm) is equal to 0.1915.

The writers calculated the temperature distributions in the Earth's troposphere with its nitrogen-oxygen composition and moderate pressure and a totally different Venus's troposphere with its carbon dioxide composition and high pressure (Table 1). As shown in this table, the values calculated using Eq. (5) are close to the temperature distribution in the standard Earth's troposphere model with an accuracy of about 0.1%. The standard Earth's atmosphere model in essence is a correlation between the temperature/pressure and elevation above the sea level averaged over the entire planet. This tropospheric model, with a gradient of 6.5 K/km, is customarily used for tuning airplane altimeters and calibration of barometers used for surface observations.

A much more rigid verification of adiabatic theory was obtained on calculating the temperature distribution in the dense (carbon dioxide) atmosphere of Venus based on its pressure and composition (temperatures on Venus were measured in the troposphere by the Soviet and American space probes).

On Venus, $p_s = 90.9$ atm and $T_s = 735.3$ K (Venus, 1989). According to Mokhov et al. (2003): $p_s = 95$ atm, $T_s = 740$ K, $S = 2.62 * 10^6$ erg/cm^2 * s, and $\psi \approx 3°$.

At an elevation of 30 km, $T_{30\,\mathrm{km}} = 496.9$ K and $p_{30\,\mathrm{km}} = 9.458$ atm, $\alpha = 0.1732$. The best fit between the empirical data and the experimental curve occurs at $\alpha = 0.1798$.

Verification of results obtained using Eq. (5) is presented in Tables 1 and 2 and Figure 4.

As shown in Table 2 and Figure 5, the theoretical temperature distribution in the troposphere of Venus is close to the empirical measurements provided in the publication entitled Venus (1989), despite the fact that Earth's parameters are used in Eq. (4). The fit to the altitude of 40 km is within 0.5°C to 1.0°C. Higher up to an altitude of up to 60 km, the theoretical temperatures lie between the two sets of empirical data. Higher, at $p < 0.2$ atm, the tropopause occurs in the troposphere of Venus, and the theory under consideration is no longer operative.

According to the greenhouse effect theory, the low concentrations of greenhouse gases for all practical purposes do not affect the tropospheric air temperature, because after the greenhouse gases absorb the IR (heat) radiation, the radiation disappears. Its energy is transferred into the energy of oscillations of air molecule. As a result, the irradiated air is heated, expands and rapidly rises to the stratosphere. There, it commingles

Table 1
Earth's troposphere temperature distribution according to the standard atmosphere model and that obtained using Eq. (5)

Standard atmospheric model				Theoretical estimation [Eq. (5)]			
h (km)	p (mm Hg)	T (°C)	T (K)		p (atm)	T (K)	T (°C)
0.0	760.00	15.00	288.00	Troposphere	1.00	288.00	15.00
0.5	716.01	11.75	284.75		0.9421	284.75	11.77
1.0	674.11	8.50	281.50		0.8870	281.50	8.50
1.5	634.21	5.25	278.25		0.8345	278.24	5.24
2.0	596.26	2.00	275.00		0.7846	275.00	2.00
2.5	560.16	−1.25	271.75		0.7371	271.24	−1.26
3.0	525.87	−4.50	268.50		0.6919	268.49	−4.51
3.5	493.30	−7.75	265.25		0.6491	265.24	−7.76
4.0	462.40	−11.00	262.00		0.6084	262.00	−11.00
4.5	433.10	−14.25	258.75		0.5699	258.75	−14.25
5.0	405.33	−17.50	255.50		0.5333	255.49	−17.51
5.5	379.04	−20.75	252.25		0.4987	252.25	−20.75
6.0	354.16	−24.00	249.00		0.4660	249.01	−23.99
6.5	330.72	−27.25	245.75		0.4345	245.51	−27.29
7.0	308.52	−30.50	242.50		0.4059	242.55	−30.45
7.5	287.55	−33.75	239.25		0.3784	239.33	−33.67
8.0	267.79	−37.00	236.00		0.3524	236.10	−36.90
8.5	249.16	−40.25	232.75		0.3278	232.87	−40.13
9.0	231.62	−43.50	229.50		0.3048	229.67	−43.33
9.5	215.09	−46.75	226.25		0.2830	226.44	−46.56
10.0	199.60	−50.00	223.00		0.2626	223.24	−49.76
10.5	185.01	−53.25	219.75		0.2434	220.03	−52.97
11.0	171.34	−56.50	216.50		0.2254	216.84	−56.16
11.5	160.11	−56.50	216.50	Tropopause	0.2107	214.07	−58.93
12.0	149.34	−56.50	216.50		0.1969	211.32	−61.68

with the thinned air and the air temperature in the troposphere declines again to the adiabatic distribution level, i.e., practically, it does not change.

A similar situation must occur when the air is heated upon condensation of water vapor. On the other hand, when the greenhouse gas concentration is substantial, the opposite scenario occurs: there is climate cooling rather than warming. If the nitrogen-oxygen Earth's atmosphere was replaced by carbon dioxide atmosphere (at the same near-surface atmospheric pressure of 1 atm), then [using Eq. (4)], the average tropospheric temperature would have declined by several degrees instead of increasing as is generally believed. This can be explained as follows: The adiabatic exponent for a carbon dioxide atmosphere $\alpha_{CO_2} = 0.1428$, which is lower than for the nitrogen-oxygen atmosphere ($\alpha_{N_2+O_2} = 0.1905$). Molar weight of carbon dioxide, on the other hand, is higher: ($\mu_{CO_2} = 44$) than that for the nitrogen-oxygen atmosphere ($\mu_{N_2+O_2} = 28.89$). Consequently, the carbon dioxide atmosphere, like a thin blanket with lower specific heat, preserves heat less than the thicker nitrogen-oxygen atmosphere with higher specific heat.

Table 2
Venus's troposphere temperature: empiric and estimated from Eq. (5)

Empirical data from "Planet Venus..."					Theoretical estimates		
h (km)	T (K)	p (bar)	T (K)	p (bar)	h (km)	p (atm)	T (K)
0	735.3	92.10			0	90.92	740.7
1	727.7	86.45			1	85.34	732.3
2	720.2	81.08			2	80.05	723.9
3	712.4	76.01			3	75.03	715.6
4	704.6	71.20			4	70.29	707.2
5	696.8	66.65			5	65.79	698.9
6	688.8	62.35			6	61.55	690.5
7	681.1	58.28			7	57.53	682.2
8	673.6	54.44			8	53.47	673.9
9	665.8	50.81			9	50.16	665.6
10	658.2	47.39			10	46.78	657.3
12	643.2	41.12			12	40.59	640.7
14	628.1	35.57			14	35.11	624.2
16	613.3	30.66			16	30.27	607.8
18	597.1	26.33			18	25.99	591.4
20	580.7	22.52			20	22.23	575
22	564.3	19.17			22	18.92	558.6
24	547.5	16.25			24	16.04	542.2
26	530.7	13.70			26	13.52	525.8
28	513.8	11.49			28	11.34	509.5
30	496.9	9.581			30	9.458	493.1
Measurement latitude: 0°–30°			Measurement latitude: 75°		Theoretical estimate		
33	471.7	7.211	471.7	7.211	33	7.118	468.5
36	448.0	5.346	446.5	5.345	36	5.277	444
39	425.1	3.903	420.5	3.894	39	3.848	419.5
42	403.5	2.802	394.5	2.78	42	2.755	395
45	385.4	1.979	368.7	1.941	45	1.935	370.7
48	366.4	1.375	343.5	1.321	48	1.331	346.6
51	342.0	0.9347	318.5	0.8741	51	0.8905	322.4
54	312.8	0.6160	290.2	0.5582	54	0.5796	298.5
57	282.5	0.3891	258.2	0.3392	57	0.3595	273.9
60	262.8	0.2357	237.5	0.1948	60	0.2125	249.2

Likewise, if the carbon dioxide atmosphere on Venus was replaced by a nitrogen-oxygen one at the same atmospheric pressure of 90.9 atm, the surface temperature would rise from the current 735 K to 777 K (463°C to 504°C). Thus, increasing saturation of atmosphere with carbon dioxide (despite its heat radiation absorbing capacity), with all other conditions being equal, results in a decrease and not an increase of the greenhouse effect and a decrease in the average temperature of planet's troposphere.

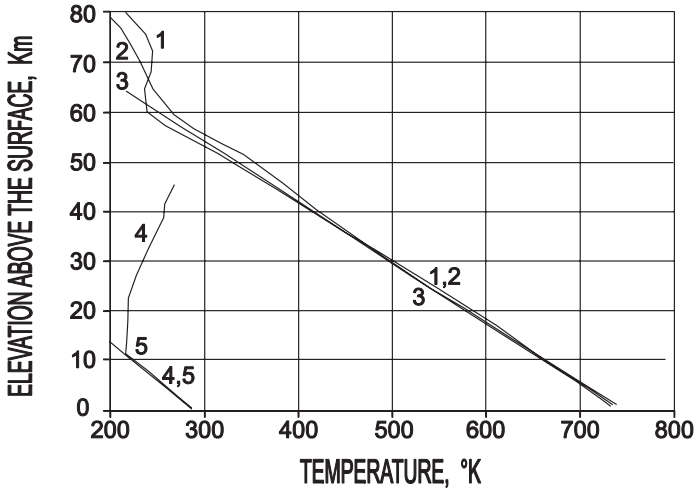

Figure 4. Temperature distribution in the Earth's troposphere and stratosphere (curve 4) and in the troposphere of Venus (curve 2, at 30° latitude, curve 1, at 75° latitude). Curves 3 and 5 are calculated based on the adiabatic theory of the greenhouse effect [Eq. (5)].

An explanation for this apparent paradox is in that the heat release from the troposphere mostly occurs through convection. Convection is much more efficient than the radiation heat transfer mechanism. Thus, as carbon dioxide concentration increases (heat radiation absorption by carbon dioxide increases as well), the convective air mass exchange increases even to a greater extent. This mass exchange releases this heat out of the troposphere.

It is possible that the increased severe weather conditions in the troposphere observed recently is due to accumulation of carbon dioxide in the atmosphere, volcanism, changes in the Sun's activity and other natural processes.

This conclusion may well be substantiated by experimental data from drilling in the Antarctic ice cover (Figure 5). Figure 5 shows that the temperature fluctuation curve runs somewhat ahead of the corresponding changes of carbon dioxide concentration. Mokhov et al. (2003) showed that changes in CO_2 concentration always occur about 500 years after peaks in Sun radiation. Thus, these drilling data show that over the 420,000 years temperature changes have always been ahead of the respective CO_2 concentration changes.

In conclusion, a common perception of climate warming as a result of CO_2 and other "greenhouse" gases accumulating in the atmosphere is a myth. In reality, CO_2 accumulation, under the same conditions, can only lead to the cooling-down of climate (also see Khilyuk and Chilingar, 2003).

The Evolution of Composition and Pressure of Earth's Atmosphere

The surface of primordial Earth was covered with a layer of ultrabasic regolite. It absorbed all chemically active gases (such as CO_2, CO, O_2, and H_2O). As a result, the atmosphere was composed of inert nitrogen with traces of noble gases, with atmospheric pressure being close to 1 atm. That is necessary for the existence at that time of an above-freezing

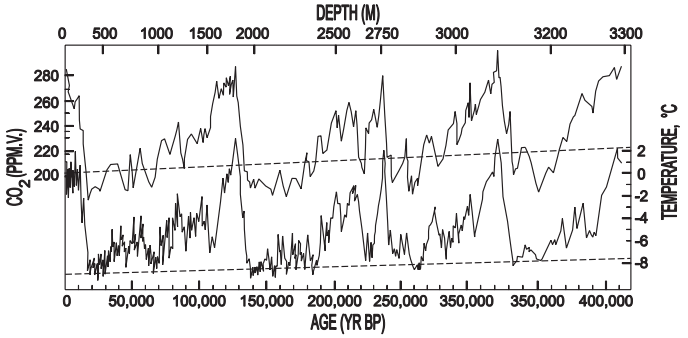

Figure 5. Comparison of CO_2 concentration changes and temperature fluctuations over the recent 420,000 years. Data collected at the Antarctic station "Vostok" (the zero year is set at the origin and increases to the right). The CO_2 and temperature data are derived from cores in a well drilled through the ice cover to TD = 3,623 m (11,886.4 ft) (after Petit et al., 1999). The temperature trend (dashed line) indicates a general cooling over the recent 420,000 years, although shorter-term temperature fluctuations reach 10°C. Mokhov et al. (2003) and Fischer at al. (1999) show that the temperature curve is ahead of CO_2 changes by about 500 to 600 years. During the cooling events, the lag in CO_2 curve (peaks in solar irradiance precede the peaks in CO_2 concentration) was even more pronounced.

temperature, which is a precondition for appearance of liquid water necessary for the emergence of life (see Sorokhtin and Ushakov, 2002).

After the Earth degassing began in Early Archaean time, the carbon dioxide and methane partial pressures rapidly increased. This was due to CO_2 reaction with the metallic iron, which was present in the primordial matter of a young Earth:

$$4Fe + 2H_2O + CO_2 \rightarrow 4FeO + CH_4 + 41.8 \text{ kcal/mole} \quad (6)$$

Also, formaldehyde, which is the primary base of many organic compounds, entered into the water:

$$2Fe + H_2O + CO_2 \rightarrow 2FeO + HCOH + 3.1 \text{ kcal/mole} \quad (7)$$

That is why initially a significantly reducing atmosphere was composed of nitrogen, carbon dioxide and methane. This, undoubtedly, facilitated the emergence of life on Earth. Due to dissociation of methane by the Sun's radiation, approximately 200 MY after beginning of the Earth's tectonic activity (about 4 BY ago), the Earth's atmosphere was converted into a neutral carbon dioxide-nitrogen one.

As shown in Figure 6, the partial pressure of carbon dioxide reached 3 to 4 atm in the Archaean time. During Proterozoic and Phanerozoic time, almost the entire carbon dioxide degassed from the mantle was tied in carbonates (C_{carb}) or biogenic matter (C_{org}). Due to small volume of water in the Archaean oceans, the mass of tied CO_2 was substantially lower than the mass of mantle-degassed CO_2, which moved into the atmosphere.

About 2.5 BY ago, after the separation of Earth's crust and the formation of serpentinite layer of oceanic crust, there was a drastic decline in tectonic activity. At that time, at the Archaean-Proterozoic boundary, a significant increase in the binding of CO_2 in carbonates occurred (Sorokhtin and Ushakov, 2002). As a result, the CO_2 partial pressure during the Early Proterozoic time dropped almost to 1 mbar. Huge amounts of carbonates

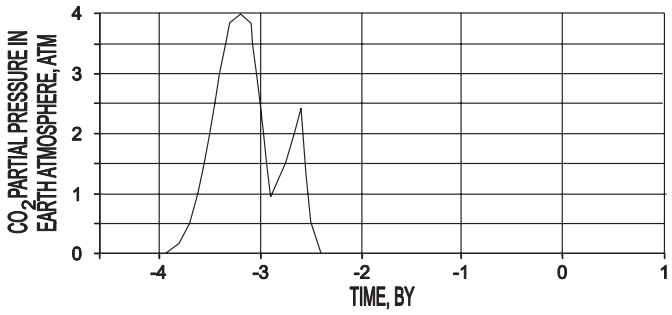

Figure 6. Evolution of partial pressure of CO_2 in the Earth's atmosphere. The graph does not show the expected increase in the partial pressure of CO_2 in the far future due to dissociation of carbon-containing compounds.

were deposited. Due to their low resistance to weathering, however, most of them were later redeposited in younger formations.

As a result of nitrogen degassing from the mantle, the partial pressure of nitrogen increased substantially during the Late Archaean time. Degassing of nitrogen (as well as degassing of other volatile atmospheric and hydrospheric components) can be described by the following equation (Sorokhtin and Ushakov, 2002):

$$m_i = (m_i)_0 * (1 - e^{-\chi z}), \tag{8}$$

where m_i is the mass of degassed volatile component (in this case, nitrogen); $(m_i)_0$ is the total mass of the ith component in the Earth; χ is the component's volatility exponent; and z is the tectonic parameter defined by the ratio of total loss of heat at depth by the Earth and its current value (which is equal to 1).

The atmospheric pressure (and hence temperature) decline during the Proterozoic and Phanerozoic time could have occurred only due to a decrease in nitrogen partial pressure. There are few bacteria that can assimilate and bind the atmospheric nitrogen into organic matter. Also, some smaller portion of nitrogen may have been bonded due to thunderstorm activities in the atmosphere. All other forms of live organisms assimilate nitrogen through the phytoplankton or plants, which, in turn, are fed by the nitrogen compounds produced by nitrogen-consuming bacteria.

It is possible to estimate the amount of nitrogen buried in the oceanic deposits using the mass of buried organic carbon (C_{org}). According to Romankevich (1984), the C_{org}/N_{org} ratio in the deposits may be close to 1/0.1. Fohr (1989) obtained a different ratio, close to 1/0.05. The writers assumed an intermediate value of that ratio: $C_{org}/N_{org} \approx$ 1/0.08. Ronov and Yaroshevsky (1978) stated that presently $3.9*10^{21}$ g of C_{org} are present in the oceanic deposits of pelagic zone and shelves plus (9.02 to 8.09) $* 10^{21}$ g, in the continental deposits. Thus, the amount of N_{org} in the present-day oceanic deposits is about $3.12 * 10^{20}$ g, whereas in the continental deposits it is about $5.0 * 10^{20}$ g.

In order to determine the N_{org} accumulation rate during the past geologic epochs the writers assumed the following: (1) the oceanic biomass was always proportional to phosphorus dissolved in water, and (2) the phosphorus concentration in water remained more or less constant (Schopf, 1980). In conclusion, the oceanic biomass is always proportional to the mass of the ocean itself. One can estimate the N_{org} mass bonded in the oceanic deposits and removed together with these deposits to the mantle through the

subduction zones (over the Earth's geologic evolution) using the following equation:

$$(\mathrm{N_{org}})^{\Sigma_{\mathrm{ocean}}} \approx \frac{(\mathrm{N_{org}})_{\mathrm{ocean}}}{(m_{w_{\mathrm{ocean}}})_0} * \int_{e=-4*10^9}^{e} m_{w_{\mathrm{ocean}}} dt, \tag{9}$$

where $(\mathrm{N_{org}})^{\Sigma_{\mathrm{ocean}}}$ is the total organic nitrogen mass removed from the ocean over the time interval from $t = -4$ BY to the present time ($t = 0$); $(\mathrm{N_{org}})_{\mathrm{ocean}}/\tau$ is the present-day rate of $\mathrm{N_{org}}$ burial in the oceanic deposits; $\tau \approx 120$ MMY (average age of the ocean floor); and $m_{w_{\mathrm{ocean}}}$ and $(m_{w_{\mathrm{ocean}}})_0$ are the current value and the present-day water mass in the World Ocean, respectively (the latter is equal to $1.37 * 10^{24}$ g).

Integration of Eq. (9) showed that over the entire period of Earth's geologic evolution (i.e., the recent 4 BY), $4.4 * 10^{21}$ g of nitrogen were removed from the atmosphere due to bonding of nitrogen by bacteria in the oceanic biota. In addition, about $5.0 * 10^{20}$ g of nitrogen was preserved in continental deposits over the recent 400 MMY.

Thus, approximately $4.9 * 10^{21}$ g of nitrogen was removed from the atmosphere over the entire period of Earth's evolution. As a result, the atmospheric pressure declined by 960 mbar (the present-day partial pressure of nitrogen is 760 mbar). The current decline in the nitrogen pressure is very small: $5.3 * 10^{-7}$ mbar/year. Over the recent billion years, however, decline in the nitrogen pressure was 440 mbar (0.44 atm).

Since the middle of Proterozoic, decline in the partial pressure of nitrogen became noticeable and was related to the activity of nitrogen-consuming bacteria (Sorokhtin, 2005b). In the Middle Proterozoic time there was no glaciation even on the continents near the poles (Chumakov, 2004), indicating that the atmospheric pressure must have been at least 1.6 atm (see Sorokhtin, 2005b; Sorokhtin and Ushakov, 2002). Using these data and the current nitrogen atmospheric pressure of 0.755 atm, it is possible to determine the nitrogen evolution in the atmosphere (Figure 7).

Simultaneously, during the Late Riphaean time (especially after the disappearance of metallic iron from Pre-Cambrian mantle), biogenic oxygen started to accumulate in the atmosphere (Sorokhtin, 2004; Sorokhtin and Ushakov, 2002) (Figure 8). This resulted

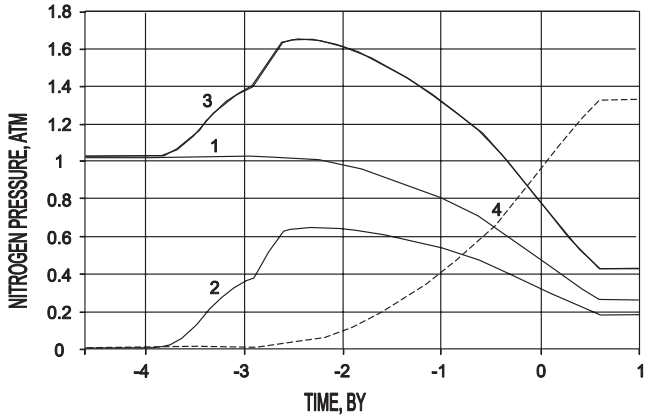

Figure 7. Origin of nitrogen in the Earth's atmosphere and its pressure evolution. (1) Nitrogen of the primordial atmosphere of young Earth. (2) Degassed mantle nitrogen. (3) Total atmospheric pressure of nitrogen. (4) Nitrogen mass removed from the atmosphere by nitrogen-consuming bacteria (converted to pressure).

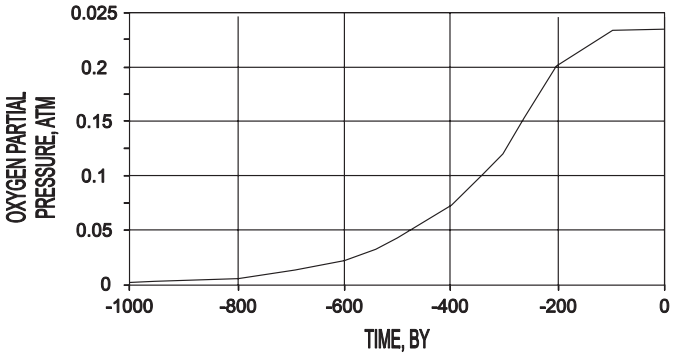

Figure 8. Oxygen partial pressure distribution over the recent 1 BY (the current partial pressure is 0.2315 atm).

in the most profound restructuring of the entire Earth's biota. There was an explosive appearance of new life forms and the emergence of multi-cellular organisms whose metabolism was based on the consumption of atmospheric oxygen.

Partial pressure of nitrogen continued its decline in Phanerozoic time, although during Paleozoic and Mesozoic time this was substantially compensated by the accelerated generation of biogenic oxygen. This phenomenon was particularly strong after the flowering plants (major oxygen generators) became common during late Mesozoic time when oxygen partial pressure reached its maximum and for a time compensated for a decline in nitrogen's pressure. After that, the partial pressure of oxygen reached a plateau (about 230 mbar). Then, due to continued biogenic decline in partial pressure of nitrogen, in the Mesozoic time the atmospheric pressure began to decrease again. According to Eq. (4), a decline in the atmospheric pressure results in the cooling-down of climate.

The nitrogen-consuming bacteria played a positive role in creating comfortable conditions for the development of a highly organized life on Earth. Without these bacteria, the current atmospheric pressure would be close to 2 atm and the average near-surface temperature would be nearly 50°C (rather than 15°C) and even over 70°C at the equator, which is above the coagulation temperature of most proteins.

Thus, the conditions suitable for a highly-organized life could have existed only at the tops of mountains located at high latitudes. This would have prevented the accumulation of sufficient oxygen to support life. In fact, should nitrogen have not been removed from the Earth's atmosphere, today (as during the Archaean time) the Earth would have been populated just by the thermophilic bacteria and, maybe, by primitive multi-cellular organisms.

The evolution of Earth's atmosphere over the entire Earth's history is presented in Figure 9. In the far future, oxygen's partial pressure would drastically increase due to abiogenic oxygen degassing from the Earth's core. Currently, the matter of the external shell of core is forming as a result of reduction of the ferrous oxide in silicates as follows:

$$2\mathrm{FeO} \rightarrow \mathrm{Fe} * \mathrm{FeO} + \mathrm{O}. \tag{10}$$

The released oxygen, in the environment of high pressure and liberated compression energy (magnetite molecules have smaller volume), combines with ferrous oxides again

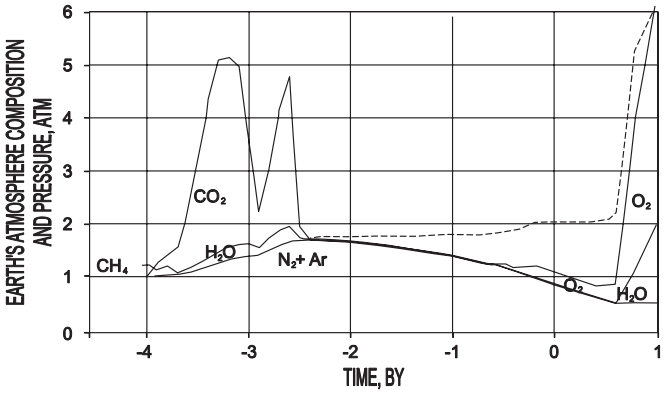

Figure 9. Evolution of the atmospheric composition and pressure of the Earth. The dashed line represents the conditions with no bacterial consumption of nitrogen (after Sorokhtin and Ushakov, 2002).

forming mantle's magnetite component:

$$3FeO + O \rightarrow Fe_3O_4 + 76.48 \text{ kcal/mole}. \tag{11}$$

After the complete oxidation of iron of mantle silicate (up to the magnetite stoichiometry), the formation of Earth's core matter would be accompanied by the release of free oxygen which is not being absorbed through any reaction:

$$2Fe_3O_4 \rightarrow 3Fe * FeO + 5O. \tag{12}$$

As a result, 600 MMY in the future, free oxygen will begin entering the atmosphere and its partial pressure will rapidly reach 10 atm. This will cause a strong greenhouse effect, giving rise to average temperatures above 180°C. After boiling-up of ocean's water, the atmospheric pressure will increase further to 270 atm and the temperatures will increase to 600°C (higher than the current temperature on Venus of 460°C).

Evolution of Earth's Climates

Sorokhtin (2001) estimated the temperatures of the past, current, and future climates of the Earth (Figure 10).

Figure 11 shows the average surface temperature distributions at the equator (curve 1), at mid-latitudes (curve 2), and at the poles (curve 3). The curves are drawn on an assumption that the latitudinal contrasts of the climate are in an inverse proportion to the atmospheric pressure. This assumption is supported by the temperature distributions discovered at different latitudes in the upper troposphere of Venus.

The Early Archaean temperatures at the poles were considerably below freezing point. At the same time, the oceans that had been located then at the equatorial belt and in low latitudes, remained warm (Sorokhtin, 2004; Sorokhtin and Ushakov, 2002).

If the temperature at the sea level is known, one can determine the temperature at any elevation for $p \geq 0.2$ atm:

$$\text{grad } T = \frac{g}{c_p}, \tag{13}$$

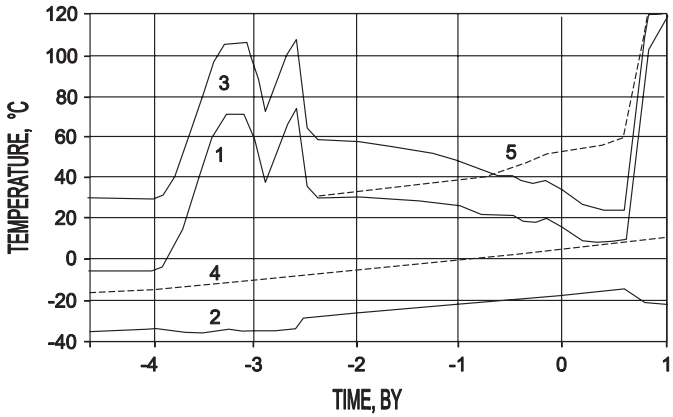

Figure 10. Averaged evolution of Earth's climates at the constant precession angle $\Psi = 24°$: (1) Earth's average surface temperature at sea level. (2) Radiation (effective) Earth's temperature as seen from the outer space. (3) Greenhouse effect of the Earth's atmosphere. (4) Temperature of absolute black body determined using Eq. (4) at the Earth's distance from the Sun indicating an increase in Sun's luminosity (S) with time. (5) Average temperature of the Earth in the absence of nitrogen consumption by bacteria.

where g is the gravitational acceleration and c_p is the specific heat, which can be determined from the Earth's atmospheric composition and pressure (see Figure 9). The level of continent stand depends on the Earth's tectonic activity and surface position of the ocean (Sorokhtin, 2004; Sorokhtin and Ushakov, 2002). The elevation of continents above the ocean level varied significantly during the geologic evolution (Figure 12). In Archaean time, there were high-intensity heat flows from the mantle. The dense lithosphere underlying the continental crust was at that time very thin. Being lighter, the continents stood high above the average level of free mantle. That is why in the Archaean time the average surface elevation of continents had been over 6 km; in the Middle Proterozoic

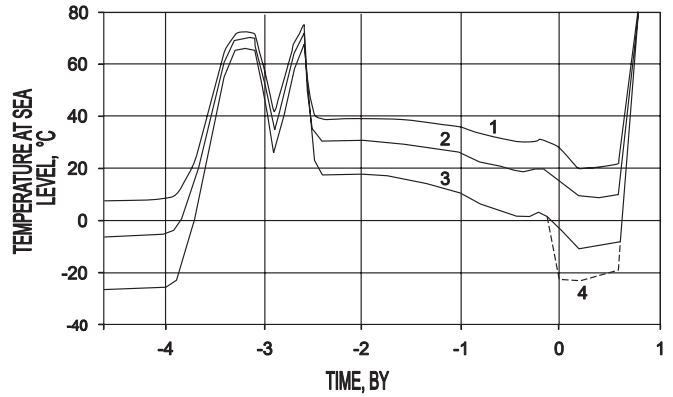

Figure 11. Evolution of averaged temperatures of Earth's surface at sea level at a fixed precession angle $\Psi = 24°$: (1) Temperature at the equator. (2) Average Earth's temperature. (3) Temperature at the poles. (4) Temperature of the ice cover in the polar oceans (taking into account the albedo of snow surface).

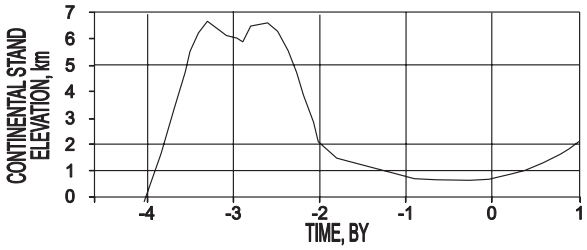

Figure 12. Evolution of the height of continents above the ocean level.

time, it decreased to 2 km; and currently, it is 600 to 800 m. In the future, some increase in the elevation of continents will occur due to decreased tectonic activity and the corresponding drop of sea level because of deepening of ocean depressions.

The temperature at sea level of polar areas with high-albedo snow cover can be determined using Eq. (14) considering their sphericity and the fact that the polar areas are illuminated by the Sun only half a year. Actually, the surface temperatures of such areas are equal to their radiation temperatures:

$$T = \left[\frac{S(1-A)}{2 * \sigma * 2 * \dfrac{1-\cos\psi}{(\sin\psi)^2}} \right]^{1/4}, \tag{14}$$

where A is the albedo of snow-covered polar areas; ψ is the Earth's precession angle; $\sigma = 5.67 * 10^{-5}$ erg/cm^2 $*$ s $*$ deg^4 is the Stephan-Boltzmann constant; S is the Sun's constant of $1.367 * 10^6$ erg/cm^2 $*$ s.

On assuming that: $\psi = 23.44°$; the average Arctic Ocean albedo $A_N = 0.66$; Central Antarctic albedo $A_A = 0.69$ (Kotlyakov, 2000) at the average temperature gradient over the Antarctic (grad T) of 8.1 K/km, the annual average temperature at the North Pole $=$ -22.8°C (empiric temperature is -23°C). Similarly determined, the temperatures in the Central Antarctic at an altitude of 1, 2, 3, and 4 km are -36.6, -44.7, -52.8, and -60.9°C, respectively.

The writers compared the calculated average temperature at the surface of Antarctic ice cover against the annual average temperatures $\overline{T}$ in the Central Antarctic (experimental measurements in wells) where marine cyclones practically never reach. Actual temperature measurements are as follows: (1) "C" Dome, elevation 3,240 m, $\overline{T} = -53$°C (Kotlyakv, 2000); (2) "Komsomolskaya" and "Vostok" stations, elevation 3,500 m, $\overline{T} = -55$°C and -55.5°C, respectively; and (3) at the top of Antarctic's main dome, $\overline{T} = -60$°C (Sorokhtin and Kapitsa, personal communication); The calculated values at the same locations are -54.9, -56.9, and -61°C, respectively, which are in close agreement with actual ones.

The calculated average temperatures at the top of continents are presented in Figure 13. Roman-numbered areas represent periods of Earth's glaciations. They are identified based on the intersection of theoretical temperature distribution curves for the continents positioned at the poles with the zero value.

Earth's glaciations must stop occurring in about 600 MMY in the future when the mantle iron is completely oxidized to the magnetite and the active degassing of endogenous oxygen according to Eq. (4) is begun.

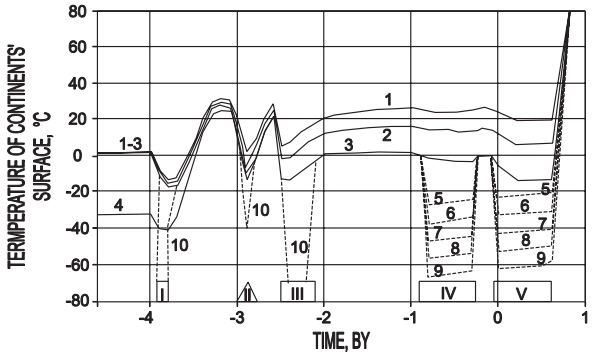

Figure 13. Average continent surface temperatures at the precession angle $\Psi \approx 24°$. Elevation of continents and the snow-cover albedo during continental glaciations are taken into account. (1) Continent temperature at the equator (elevation of continents is taken into account). (2) Average temperature of continents. (3) Surface temperature of the continents that were located at the poles during Proterozoic and Mesozoic time (elevation of continents is taken into account). (4) Young Earth temperature at the poles. (5)–(9) Ice cover temperature at the elevations of 0, 1, 2, 3, and 4 km, respectively (snow-cover albedo is assumed to be equal to about 0.7). (10) Surface temperature of the Huron ice cover and Archaean ice covers at the elevations of 3 and 6 km, respectively. Areas I through V are technically ($T_{\text{cont}} \leq 0$) identified as glaciation periods on the continents that drifted into high latitudes.

Precession Cycles and Earth's Ice Periods

Precession occurs because the distribution of Earth's mass deviates from the spherical symmetry. This deviation is caused primarily by the position of continents and oceans on the globe. The Earth's orbit precession cycles in its revolution around the Sun (so-called Milankovic cycles) are superimposed on the Earth's precession.

Summary and Conclusions

Inspection of the changes in global atmospheric temperature during the last 1,000 years shows that the global temperature dropped about 2°C over the last millennium. Thus, we live in a cooling geologic epoch and the global warming observed during the last 150 years is only a short episode in the geologic history. The current global warming is probably due to increased solar and tectonic activities.

Global climate changes occur continuously and naturally at various scales of intensity, duration and direction. Geologists view these changes in context of time and intensity at scales much longer than human history (see Gerhard, 2004).

Current theories of human-induced greenhouse climate change tend to ignore longer-term climate history. Instead, they are focused on the results of computer models, which are predicated on the greenhouse gases being the significant driver of climate change.

References and Bibliography

Arrhenius, S. 1896. On the influence of carbonic acid in the air upon the temperature of the ground. *Phil. Mag.* 41:237–276.

Bachall, J. N. 1982. Standard solar models and the uncertainties in predicted capture rates of solar neutrinos. *Rev. Modern Physics* 54:767–799.

Budyko, M. I. 1997. *Carbon Dioxide Problem*. Leningrad: Gidrometeoizdat, 60 pp.

Chumakov, N. M. 2004a. Climatic zones and the climate of the Cretaceous period. In *Climate during the Major Biospheric Restructuring Epochs*. Moscow: Nauka, 105–123.

Chumakov, N. M. 2004b. Glacial and non-glacial climate in Pre-Cambrian. In *Climate during the Major Biospheric Restructuring Epochs*. Moscow: Nauka, 259–270.

Fischer, H., Wahlen, M., Smith, J., Mastroianni, D., and Deck, B. 1999. Ice core records of atmospheric CO_2 around the last three glacial terminations. *Science* 283:1712–1714.

Fohr, G. 1989. *Basics of Isotope Geology*. Moscow: Mir, 590 pp.

Friis-Christensen, E., and Lassen, K. 1991. Length of the solar cycle: An indicator of solar activity closely associated with climate. *Science* 254:698–700.

Gerhard, L. C. 2004. Climate change: Conflict of observational science, theory and politics. *Am. Ass. Petrol. Geol. Bull.* 88:1211–1220.

Global Warming. 1990. *The Greenpeace Report*. Oxford: Oxford University Press, 554 pp.

Greenhouse Effect. 1989. *Climate and Ecosystem Changes*. Leningrad: Gidrometeoizdat, 558 pp.

Holland, H. D. 1984. *The Chemical Evolution of Atmosphere and Ocean*. Princeton, NJ: Princeton Univ. Press.

Keigwin, L.D. 1996. The little Ice Age and Medieval Warm period in the Sargasso Sea. *Science* 274:1504–1508

Khilyuk, L. F., and Chilingar, G. V. 2003. Global warming: Are we confusing cause and effect? *Energy Sources* 25:357–370.

Khilyuk, L. F., and Chilingar, G. V. 2004. Global warming and long-term climate changes: A progress report. *Environ. Geol.* 46:970–979.

Khilyuk, L. F., and Chilingar, G. V. 2006. On global forces of nature driving the Earth's climate. Are humans involved? *Environ. Geol.* 50:899–910.

Knauth, L. P., and Lowe, D. R. 1978. Oxygen isotope geochemistry of cherts from the Onverwacht Group, 3.4 billion years, Transvaal, South Africa, with implications for secular variations in the isotopic composition of cherts. *Earth Planet. Sci. Lett.* 41:209–222.

Kotlyakov, V. M. 2000. *Glaciology of the Antarctic*. Moscow: Nauka, 432 pp.

Kotlyakov, V. M. 2002. *In the World of Snow and Ice*. Moscow: Nauka, 384 pp.

Landscheidt, T., 1995. Global warming or little Ice Age? In *Holocene Cycles*. A Jubilee volume in celebration of the 80th birthday of Rhodes W. Fairbridge. Finkl, C. W. (Ed.). Fort Lauderdale: The Coastal Education and Research Foundation, CERF, 371–382.

Landscheidt, T. 2003. New little ice age instead of global warming? *Energy Environ.* 14:327–350.

Lassen, K. 2000. Long-term variations in solar activity and their apparent effect on the Earth's climate. *Danish Meteorological Institute, Solar-Terrestrial Physics Division*, Lyngbyvej, 100, DK-2100 Copenhagen, 2, Denmark.

Marov, M. Ya. 1986. *Planets of the Solar System*. Moscow: Nauka, 320 pp.

Mokhov, N. N., et al. 2003. Milankovic cycles and climatic regime and atmosphere composition based on ice cores from Antarctic Station Vostok. *Materials Glaciological Investigations* 95: 3–8.

Perry, E.C., Jr., 1967. The oxygen isotope chemistry of ancient cherts. *Planet Earth. Sci. Lett*. 3:62.

Perry, E. C., Jr., and Tan, F. C. 1972. Significance of oxygen and carbon isotope determinations in Early Precambrian cherts and carbonate rocks of Southern Africa. *Bull. Geol. Soc. America* 83:647–664.

Petit, J. R., Jouzel, J., Raynaud, D., et al. 1999. Climate and atmospheric history of the past 420,000 years from the Vostok Ice Core, Antarctica. *Nature* 399:429–438.

Robinson, A. B., Baliunas, S. L., Soon, W., and Robinson, Z. W. 1998. Environmental effects of increased atmospheric carbon dioxide. Petition Project, PO Box 1925, La Jolla CA 92038-1925, [info@oism.org; info@marshall.org].

Romankevich, E. A. 1984. *Geochemistry of Organic Matter in the Ocean*. Springer Verlag, Berlin, 334 pp.

Ronov, A. B., and Yaroshevsky, A. A. 1978. Chemical composition of the Earth crust and of its shells. In *Tectonosphere of the Earth*. Moscow: Nedra, 376–402.

Schopf, T. 1980. *Paleoceanography*. Cambridge: Harvard Univ. Press.
Sorokhtin, O. G. 2001. The greenhouse effect: Myth and reality. *Herald of RAEN* 1:6–21.
Sorokhtin, O. G. 2004. Global evolution of the Earth. *Herald of RAEN* 4:3–16.
Sorokhtin, O. G. 2005a. Precession of the Earth and Pleistocene climatic cycles. *Proc. RAN* 405.
Sorokhtin, O. G. 2005b. Role of nitrogen-consuming bacteria in the emergence of Earth's glaciations. *Proc. (Doklady) RAN (Russ. Acad. Sci.)* 403:689–692.
Sorokhtin, O. G., and Ushakov, S. A. 2002. *Evolution of the Earth*. Moscow University Publishers, 560 pp.
Venus (Atmosphere, Surface and Ecosystem). 1989. Moscow: Nauka Publishers, 482 pp (in Russian).
Zachos, J., Pagani, M., Sloan, L., Thomas, E., and Billups, K. 2001. Trends, rhythms, and aberrations in global climate 65 Ma to present. *Science* 292:686–693.